
Applied Superconductivity:

Josephson Effect and Superconducting Electronics

**Manuscript to the Lectures during WS 2003/2004, WS 2005/2006, WS 2006/2007,
WS 2007/2008, WS 2008/2009, and WS 2009/2010**

Prof. Dr. Rudolf Gross

and

Dr. Achim Marx

Walther-Meißner-Institut
Bayerische Akademie der Wissenschaften
and

Lehrstuhl für Technische Physik (E23)
Technische Universität München

Walther-Meißner-Strasse 8
D-85748 Garching
Rudolf.Gross@wmi.badw.de

Contents

Preface	xxi
I Foundations of the Josephson Effect	1
1 Macroscopic Quantum Phenomena	3
1.1 The Macroscopic Quantum Model	3
1.1.1 Coherent Phenomena in Superconductivity	3
1.1.2 Macroscopic Quantum Currents in Superconductors	12
1.1.3 The London Equations	18
1.2 Flux Quantization	24
1.2.1 Flux and Fluxoid Quantization	26
1.2.2 Experimental Proof of Flux Quantization	28
1.2.3 Additional Topic: Rotating Superconductor	30
1.3 Josephson Effect	32
1.3.1 The Josephson Equations	33
1.3.2 Josephson Tunneling	37
2 JJs: The Zero Voltage State	43
2.1 Basic Properties of Lumped Josephson Junctions	44
2.1.1 The Lumped Josephson Junction	44
2.1.2 The Josephson Coupling Energy	45
2.1.3 The Superconducting State	47
2.1.4 The Josephson Inductance	49
2.1.5 Mechanical Analogs	49
2.2 Short Josephson Junctions	50
2.2.1 Quantum Interference Effects – Short Josephson Junction in an Applied Magnetic Field	50

2.2.2	The Fraunhofer Diffraction Pattern	54
2.2.3	Determination of the Maximum Josephson Current Density	58
2.2.4	Additional Topic: Direct Imaging of the Supercurrent Distribution	62
2.2.5	Additional Topic: Short Josephson Junctions: Energy Considerations	63
2.2.6	The Motion of Josephson Vortices	65
2.3	Long Josephson Junctions	68
2.3.1	The Stationary Sine-Gordon Equation	68
2.3.2	The Josephson Vortex	70
2.3.3	Junction Types and Boundary Conditions	73
2.3.4	Additional Topic: Josephson Current Density Distribution and Maximum Josephson Current	79
2.3.5	The Pendulum Analog	84
3	JJs: The Voltage State	89
3.1	The Basic Equation of the Lumped Josephson Junction	90
3.1.1	The Normal Current: Junction Resistance	90
3.1.2	The Displacement Current: Junction Capacitance	92
3.1.3	Characteristic Times and Frequencies	93
3.1.4	The Fluctuation Current	94
3.1.5	The Basic Junction Equation	96
3.2	The Resistively and Capacitively Shunted Junction Model	97
3.2.1	Underdamped and Overdamped Josephson Junctions	100
3.3	Response to Driving Sources	102
3.3.1	Response to a dc Current Source	102
3.3.2	Response to a dc Voltage Source	107
3.3.3	Response to ac Driving Sources	107
3.3.4	Photon-Assisted Tunneling	112
3.4	Additional Topic: Effect of Thermal Fluctuations	115
3.4.1	Underdamped Junctions: Reduction of I_c by Premature Switching	117
3.4.2	Overdamped Junctions: The Ambegaokar-Halperin Theory	118
3.5	Secondary Quantum Macroscopic Effects	122
3.5.1	Quantum Consequences of the Small Junction Capacitance	122

3.5.2	Limiting Cases: The Phase and Charge Regime	125
3.5.3	Coulomb and Flux Blockade	128
3.5.4	Coherent Charge and Phase States	130
3.5.5	Quantum Fluctuations	132
3.5.6	Macroscopic Quantum Tunneling	133
3.6	Voltage State of Extended Josephson Junctions	139
3.6.1	Negligible Screening Effects	139
3.6.2	The Time Dependent Sine-Gordon Equation	140
3.6.3	Solutions of the Time Dependent Sine-Gordon Equation	141
3.6.4	Additional Topic: Resonance Phenomena	144
II	Applications of the Josephson Effect	153
4	SQUIDS	157
4.1	The dc-SQUID	159
4.1.1	The Zero Voltage State	159
4.1.2	The Voltage State	164
4.1.3	Operation and Performance of dc-SQUIDS	168
4.1.4	Practical dc-SQUIDS	172
4.1.5	Read-Out Schemes	176
4.2	Additional Topic: The rf-SQUID	180
4.2.1	The Zero Voltage State	180
4.2.2	Operation and Performance of rf-SQUIDS	182
4.2.3	Practical rf-SQUIDS	186
4.3	Additional Topic: Other SQUID Configurations	188
4.3.1	The DROS	188
4.3.2	The SQIF	189
4.3.3	Cartwheel SQUID	189
4.4	Instruments Based on SQUIDS	191
4.4.1	Magnetometers	192
4.4.2	Gradiometers	194
4.4.3	Susceptometers	196

4.4.4	Voltmeters	197
4.4.5	Radiofrequency Amplifiers	198
4.5	Applications of SQUIDs	200
4.5.1	Biomagnetism	200
4.5.2	Nondestructive Evaluation	204
4.5.3	SQUID Microscopy	206
4.5.4	Gravity Wave Antennas and Gravity Gradiometers	208
4.5.5	Geophysics	210
5	Digital Electronics	215
5.1	Superconductivity and Digital Electronics	216
5.1.1	Historical development	217
5.1.2	Advantages and Disadvantages of Josephson Switching Devices	219
5.2	Voltage State Josephson Logic	222
5.2.1	Operation Principle and Switching Times	222
5.2.2	Power Dissipation	225
5.2.3	Switching Dynamics, Global Clock and Punchthrough	226
5.2.4	Josephson Logic Gates	228
5.2.5	Memory Cells	234
5.2.6	Microprocessors	236
5.2.7	Problems of Josephson Logic Gates	237
5.3	RSFQ Logic	239
5.3.1	Basic Components of RSFQ Circuits	241
5.3.2	Information in RSFQ Circuits	246
5.3.3	Basic Logic Gates	247
5.3.4	Timing and Power Supply	249
5.3.5	Maximum Speed	249
5.3.6	Power Dissipation	250
5.3.7	Prospects of RSFQ	250
5.3.8	Fabrication Technology	253
5.3.9	RSFQ Roadmap	254
5.4	Analog-to-Digital Converters	255
5.4.1	Additional Topic: Foundations of ADCs	256
5.4.2	The Comparator	261
5.4.3	The Aperture Time	263
5.4.4	Different Types of ADCs	264

6	The Josephson Voltage Standard	269
6.1	Voltage Standards	270
6.1.1	Standard Cells and Electrical Standards	270
6.1.2	Quantum Standards for Electrical Units	271
6.2	The Josephson Voltage Standard	274
6.2.1	Underlying Physics	274
6.2.2	Development of the Josephson Voltage Standard	274
6.2.3	Junction and Circuit Parameters for Series Arrays	279
6.3	Programmable Josephson Voltage Standard	281
6.3.1	Pulse Driven Josephson Arrays	283
7	Superconducting Photon and Particle Detectors	285
7.1	Superconducting Microwave Detectors: Heterodyne Receivers	286
7.1.1	Noise Equivalent Power and Noise Temperature	286
7.1.2	Operation Principle of Mixers	287
7.1.3	Noise Temperature of Heterodyne Receivers	290
7.1.4	SIS Quasiparticle Mixers	292
7.1.5	Josephson Mixers	296
7.2	Superconducting Microwave Detectors: Direct Detectors	297
7.2.1	NEP of Direct Detectors	298
7.3	Thermal Detectors	300
7.3.1	Principle of Thermal Detection	300
7.3.2	Bolometers	302
7.3.3	Antenna-Coupled Microbolometers	307
7.4	Superconducting Particle and Single Photon Detectors	314
7.4.1	Thermal Photon and Particle Detectors: Microcalorimeters	314
7.4.2	Superconducting Tunnel Junction Photon and Particle Detectors	318
7.5	Other Detectors	328
8	Microwave Applications	329
8.1	High Frequency Properties of Superconductors	330
8.1.1	The Two-Fluid Model	330
8.1.2	The Surface Impedance	333
8.2	Superconducting Resonators and Filters	336
8.3	Superconducting Microwave Sources	337

9 Superconducting Quantum Bits	339
9.1 Quantum Bits and Quantum Computers	341
9.1.1 Quantum Bits	341
9.1.2 Quantum Computing	343
9.1.3 Quantum Error Correction	346
9.1.4 What are the Problems?	348
9.2 Implementation of Quantum Bits	349
9.3 Why Superconducting Qubits	352
9.3.1 Superconducting Island with Leads	352
III Anhang	355
A The Josephson Equations	357
B Imaging of the Maximum Josephson Current Density	361
C Numerical Iteration Method for the Calculation of the Josephson Current Distribution	363
D Photon Noise	365
I Power of Blackbody Radiation	365
II Noise Equivalent Power	367
E Qubits	369
I What is a quantum bit ?	369
I.1 Single-Qubit Systems	369
I.2 The spin-1/2 system	371
I.3 Two-Qubit Systems	372
II Entanglement	373
III Qubit Operations	375
III.1 Unitarity	375
III.2 Single Qubit Operations	375
III.3 Two Qubit Operations	376
IV Quantum Logic Gates	377
IV.1 Single-Bit Gates	377
IV.2 Two Bit Gates	379
V The No-Cloning Theorem	384
VI Quantum Complexity	385
VII The Density Matrix Representation	385

F	Two-Level Systems	389
I	Introduction to the Problem	389
I.1	Relation to Spin-1/2 Systems	390
II	Static Properties of Two-Level Systems	390
II.1	Eigenstates and Eigenvalues	390
II.2	Interpretation	391
II.3	Quantum Resonance	394
III	Dynamic Properties of Two-Level Systems	395
III.1	Time Evolution of the State Vector	395
III.2	The Rabi Formula	395
G	The Spin 1/2 System	399
I	Experimental Demonstration of Angular Momentum Quantization	399
II	Theoretical Description	401
II.1	The Spin Space	401
III	Evolution of a Spin 1/2 Particle in a Homogeneous Magnetic Field	402
IV	Spin 1/2 Particle in a Rotating Magnetic Field	404
IV.1	Classical Treatment	404
IV.2	Quantum Mechanical Treatment	406
IV.3	Rabi's Formula	407
H	Literature	409
I	Foundations of Superconductivity	409
I.1	Introduction to Superconductivity	409
I.2	Early Work on Superconductivity and Superfluidity	410
I.3	History of Superconductivity	410
I.4	Weak Superconductivity, Josephson Effect, Flux Structures	410
II	Applications of Superconductivity	411
II.1	Electronics, Sensors, Microwave Devices	411
II.2	Power Applications, Magnets, Transportation	412
II.3	Superconducting Materials	412
I	SI-Einheiten	413
I	Geschichte des SI Systems	413
II	Die SI Basiseinheiten	415
III	Einige von den SI Einheiten abgeleitete Einheiten	416
IV	Vorsätze	418
V	Abgeleitete Einheiten und Umrechnungsfaktoren	419

J Physikalische Konstanten**425**

List of Figures

1.1	Meissner-Effect	19
1.2	Current transport and decay of a supercurrent in the Fermi sphere picture	20
1.3	Stationary Quantum States	24
1.4	Flux Quantization in Superconductors	25
1.5	Flux Quantization in a Superconducting Cylinder	27
1.6	Experiment by Doll and Naebauer	29
1.7	Experimental Proof of Flux Quantization	29
1.8	Rotating superconducting cylinder	31
1.9	The Josephson Effect in weakly coupled superconductors	32
1.10	Variation of n_s^* and γ across a Josephson junction	35
1.11	Schematic View of a Josephson Junction	36
1.12	Josephson Tunneling	39
2.1	Lumped Josephson Junction	45
2.2	Coupling Energy and Josephson Current	46
2.3	The Tilted Washboard Potential	48
2.4	Extended Josephson Junction	51
2.5	Magnetic Field Dependence of the Maximum Josephson Current	55
2.6	Josephson Current Distribution in a Small Josephson Junction for Various Applied Magnetic Fields	56
2.7	Spatial Interference of Macroscopic Wave Funktionen	57
2.8	The Josephson Vortex	57
2.9	Gaussian Shaped Josephson Junction	59
2.10	Comparison between Measurement of Maximum Josephson Current and Optical Diffraction Experiment	60
2.11	Supercurrent Auto-correlation Function	61
2.12	Magnetic Field Dependence of the Maximum Josephson Current of a YBCO-GBJ	63

2.13	Motion of Josephson Vortices	66
2.14	Magnetic Flux and Current Density Distribution for a Josephson Vortex	70
2.15	Classification of Junction Types: Overlap, Inline and Grain Boundary Junction	74
2.16	Geometry of the Asymmetric Inline Junction	77
2.17	Geometry of Mixed Overlap and Inline Junctions	78
2.18	The Josephson Current Distribution of a Long Inline Junction	80
2.19	The Maximum Josephson Current as a Function of the Junction Length	81
2.20	Magnetic Field Dependence of the Maximum Josephson Current and the Josephson Current Density Distribution in an Overlap Junction	83
2.21	The Maximum Josephson Current as a Function of the Applied Field for Overlap and Inline Junctions	84
3.1	Current-Voltage Characteristic of a Josephson tunnel junction	91
3.2	Equivalent circuit for a Josephson junction including the normal, displacement and fluctuation current	92
3.3	Equivalent circuit of the Resistively Shunted Junction Model	97
3.4	The Motion of a Particle in the Tilt Washboard Potential	98
3.5	Pendulum analogue of a Josephson junction	99
3.6	The IVCs for Underdamped and Overdamped Josephson Junctions	101
3.7	The time variation of the junction voltage and the Josephson current	103
3.8	The RSJ model current-voltage characteristics	105
3.9	The RCSJ Model IVC at Intermediate Damping	107
3.10	The RCJ Model Circuit for an Applied dc and ac Voltage Source	108
3.11	Overdamped Josephson Junction driven by a dc and ac Voltage Source	110
3.12	Overdamped Josephson junction driven by a dc and ac Current Source	111
3.13	Shapiro steps for under- and overdamped Josephson junction	112
3.14	Photon assisted tunneling	113
3.15	Photon assisted tunneling in SIS Josephson junction	113
3.16	Thermally Activated Phase Slippage	116
3.17	Temperature Dependence of the Thermally Activated Junction Resistance	119
3.18	RSJ Model Current-Voltage Characteristics Including Thermally Activated Phase Slippage	120
3.19	Variation of the Josephson Coupling Energy and the Charging Energy with the Junction Area	124
3.20	Energy diagrams of an isolated Josephson junction	127
3.21	The Coulomb Blockade	128

3.22	The Phase Blockade	129
3.23	The Cooper pair box	131
3.24	Double well potential for the generation of phase superposition states	132
3.25	Macroscopic Quantum Tunneling	134
3.26	Macroscopic Quantum Tunneling at Large Damping	138
3.27	Mechanical analogue for phase dynamics of a long Josephson junction	141
3.28	The Current Voltage Characteristic of an Underdamped Long Josephson Junction	145
3.29	Zero field steps in IVCs of an annular Josephson junction	147
4.1	The dc-SQUID	160
4.2	Maximum Supercurrent versus Applied Magnetic Flux for a dc-SQUID at Weak Screening	162
4.3	Total Flux versus Applied Magnetic Flux for a dc SQUID at $\beta_L > 1$	163
4.4	Current-voltage Characteristics of a dc-SQUID at Negligible Screening	165
4.5	The pendulum analogue of a dc SQUID	167
4.6	Principle of Operation of a dc-SQUID	169
4.7	Energy Resolution of dc-SQUIDs	172
4.8	The Practical dc-SQUID	173
4.9	Geometries for thin film SQUID washers	174
4.10	Flux focusing effect in a $\text{YBa}_2\text{Cu}_3\text{O}_{7-\delta}$ washer	175
4.11	The Washer dc-SQUID	176
4.12	The Flux Modulation Scheme for a dc-SQUID	177
4.13	The Modulation and Feedback Circuit of a dc-SQUID	178
4.14	The rf-SQUID	180
4.15	Total flux versus applied flux for a rf-SQUID	182
4.16	Operation of rf-SQUIDs	183
4.17	Tank voltage versus rf-current for a rf-SQUID	184
4.18	High T_c rf-SQUID	187
4.19	The double relaxation oscillation SQUID (DROS)	188
4.20	The Superconducting Quantum Interference Filter (SQIF)	190
4.21	Input Antenna for SQUIDs	191
4.22	Various types of thin film SQUID magnetometers	193
4.23	Magnetic noise signals	194
4.24	Magnetically shielded room	195
4.25	Various gradiometers configurations	196

4.26	Miniature SQUID Susceptometer	197
4.27	SQUID Radio-frequency Amplifier	198
4.28	Multichannel SQUID Systems	201
4.29	Magnetocardiography	203
4.30	Magnetic field distribution during R peak	204
4.31	SQUID based nondestructive evaluation	205
4.32	Scanning SQUID microscopy	207
4.33	Scanning SQUID microscopy images	208
4.34	Gravity wave antenna	209
4.35	Gravity gradiometer	210
5.1	Cryotron	217
5.2	Josephson Cryotron	218
5.3	Device performance of Josephson devices	220
5.4	Principle of operation of a Josephson switching device	222
5.5	Output current of a Josephson switching device	224
5.6	Threshold characteristics for a magnetically and directly coupled gate	229
5.7	Three-junction interferometer gate	230
5.8	Current injection device	230
5.9	Josephson Atto Weber Switch (JAWS)	231
5.10	Direct coupled logic (DCL) gate	231
5.11	Resistor coupled logic (RCL) gate	232
5.12	4 junction logic (4JL) gate	232
5.13	Non-destructive readout memory cell	234
5.14	Destructive read-out memory cell	235
5.15	4 bit Josephson microprocessor	237
5.16	Josephson microprocessor	238
5.17	Comparison of latching and non-latching Josephson logic	240
5.18	Generation of SFQ Pulses	242
5.19	dc to SFQ Converter	243
5.20	Basic Elements of RSFQ Circuits	244
5.21	RSFQ memory cell	245
5.22	RSFQ logic	246
5.23	RSFQ OR and AND Gate	247

5.24	RSFQ NOT Gate	248
5.25	RSFQ Shift Register	249
5.26	RSFQ Microprocessor	253
5.27	RSFQ roadmap	254
5.28	Principle of operation of an analog-to-digital converter	256
5.29	Analog-to-Digital Conversion	257
5.30	Semiconductor and Superconductor Comparators	262
5.31	Incremental Quantizer	263
5.32	Flash-type ADC	265
5.33	Counting-type ADC	266
6.1	Weston cell	271
6.2	The metrological triangle for the electrical units	273
6.3	IVC of an underdamped Josephson junction under microwave irradiation	275
6.4	International voltage comparison between 1920 and 2000	276
6.5	One-Volt Josephson junction array	277
6.6	Josephson series array embedded into microwave stripline	278
6.7	Microwave design of Josephson voltage standards	279
6.8	Adjustment of Shapiro steps for a series array Josephson voltage standard	281
6.9	IVC of overdamped Josephson junction with microwave irradiation	282
6.10	Programmable Josephson voltage standard	283
7.1	Block diagram of a heterodyne receiver	288
7.2	Ideal mixer as a switch	288
7.3	Current response of a heterodyne mixer	289
7.4	IVCs and IF output power of SIS mixer	290
7.5	Optimum noise temperature of a SIS quasiparticle mixer	293
7.6	Measured DSB noise temperature of a SIS quasiparticle mixers	294
7.7	High frequency coupling schemes for SIS mixers	295
7.8	Principle of thermal detectors	301
7.9	Operation principle of superconducting transition edge bolometer	302
7.10	Sketch of a HTS bolometer	305
7.11	Specific detectivity of various bolometers	305
7.12	Relaxation processes in a superconductor after energy absorption	307
7.13	Antenna-coupled microbolometer	308

7.14	Schematic illustration of the hot electron bolometer mixer	309
7.15	Hot electron bolometer mixers with different antenna structures	311
7.16	Transition-edge sensors	315
7.17	Transition-edge sensors	317
7.18	Functional principle of a superconducting tunnel junction detector	319
7.19	Circuit diagram of a superconducting tunnel junction detector	319
7.20	Energy resolving power of STJDs	321
7.21	Quasiparticle tunneling in SIS junctions	323
7.22	Quasiparticle trapping in STJDs	326
7.23	STJDs employing lateral quasiparticle trapping	326
7.24	Superconducting tunnel junction x-ray detector	327
8.1	Equivalent circuit for the two-fluid model	332
8.2	Characteristic frequency regimes for a superconductor	332
8.3	Surface resistance of Nb and Cu	335
9.1	Konrad Zuse 1945	341
9.2	Representation of a Qubit State as a Vector on the Bloch Sphere	342
9.3	Operational Scheme of a Quantum Computer	344
9.4	Quantum Computing: What's it good for?	345
9.5	Shor, Feynman, Bennett and Deutsch	346
9.6	Qubit Realization by Quantum Mechanical Two level System	349
9.7	Use of Superconductors for Qubits	352
9.8	Superconducting Island with Leads	354
E.1	The Bloch Sphere S^2	370
E.2	The Spin-1/2 System	371
E.3	Entanglement – an artist's view.	373
E.4	Classical Single-Bit Gate	377
E.5	Quantum NOT Gate	378
E.6	Classical Two Bit Gate	380
E.7	Reversible and Irreversible Logic	380
E.8	Reversible Classical Logic	381
E.9	Reversible XOR (CNOT) and SWAP Gate	382
E.10	The Controlled U Gate	382

E.11	Density Matrix for Pure Single Qubit States	386
E.12	Density Matrix for a Coherent Superposition of Single Qubit States	387
F.1	Energy Levels of a Two-Level System	392
F.2	The Benzene Molecule	394
F.3	Graphical Representation of the Rabi Formula	396
G.1	The Larmor Precession	400
G.2	The Rotating Reference Frame	404
G.3	The Effective Magnetic Field in the Rotating Reference Frame	405
G.4	Rabi's Formula for a Spin 1/2 System	408

List of Tables

5.1	Switching delay and power dissipation for various types of logic gates.	233
5.2	Josephson 4 kbit RAM characteristics (organization: 4096 word × 1 bit, NEC).	236
5.3	Performance of various logic gates	237
5.4	Possible applications of superconductor digital circuits (source: SCENET 2001).	251
5.5	Performance of various RSFQ based circuits.	252
7.1	Characteristic materials properties of some superconductors	325
8.1	Important high-frequency characteristic of superconducting and normal conducting . . .	334
E.1	Successive measurements on a two-qubit state showing the results A and B with the corresponding probabilities $P(A)$ and $P(B)$ and the remaining state after the measurement. . . .	373

Chapter 6

The Josephson Voltage Standard

The realization of Josephson voltage standard is one of the successful applications of the Josephson effect. It is based on the voltage-frequency relation $V = \frac{h}{2e}f = \Phi_0 f$. Therefore, defining the unit 1 V on the basis of the Josephson effect reduces the calibration of a voltage to the determination of a frequency and the knowledge of the ratio $h/2e$ of the Plank's constant and twice the elementary charge. Since the frequency can be determined with extreme accuracy by the standard of an atomic caesium clock, only a convention for the value of $\Phi_0 = h/2e$ is needed to obtain a very good reproducibility of the voltage calibration. Based on this idea the development of a Josephson voltage standard was started already in the 1970s. After overcoming some technical difficulties the Josephson effect based voltage standards are used as primary standards in the national calibration laboratories since 1990. Meanwhile even industrial companies are using these standards. Since the Josephson voltage standards have no competitors in semiconductor electronics, they represent a successful application of the Josephson effect.

6.1 Voltage Standards

6.1.1 Standard Cells and Electrical Standards

For a long period electrochemical cells were used for establishing reference voltages. Initially, these cells were mainly used to provide reliable sources of electrical current. For example, following the ideas of **Galvani**,¹ **Volta** built the first practical electrochemical cell in 1794. These cells had been the only reliable sources for electrical current for more than 50 years.²

Only after the introduction of the **Zn-Cu Daniell cell** in 1836,^{3,4} electrochemical cells were used as stable voltage sources for maintaining and disseminating the unit volt. There was a large effort in the late 19th and the early 20th century to establish a standard for electromotive force (emf) based on electrochemical reactions within chemical cells. For example, the first legal unit of voltage for the United States was based on the **Zn-Hg Clark cell**, developed by **Latimer Clark** in 1872, with its output assigned a value of 1.434 international volts by the 1893 International Electric Congress. Public Law 105, passed by the U.S. Congress in 1894, made this the legal standard of voltage in the U.S. During the years between 1893 and 1905, the standard cell devised by **Edward Weston**⁵ (Cd(Hg)/CdSO₄(aq), Hg₂S₄/Hg battery, see Fig. 6.1) was found to have many advantages over the Clark cell.⁶ The **Cd-Hg Weston cell** consists of a cadmium amalgam anode and a mercury-mercurous sulfate cathode with a saturated cadmium sulfate solution as the electrolyte. It has a much better long-term stability, a smaller temperature coefficient and less hysteresis. Furthermore, its output voltage of 1.0186 V was a better approximation to 1 V. In 1908, at the London International Conference on Electrical Units and Standards, the Weston cell was officially adopted for maintaining the volt. Due to the improved electrochemical cells in 1910 the Rayleigh Committee recommended a more precise value for the maintenance of the volt. Similar improvements had been adopted for the ampère and the ohm at the London Conference two years earlier. The newly recommended units were called **International Units**.

The Weston standard cell is sensitive to external parameters such as motion during transport, change in temperature or a small electrical current. When at times it was necessary to eliminate cells – due to changes in emf of a cell relative to the mean of the group – new cells could be added. In 1965 the National Reference Group of standard cells⁷ included 11 cells made in 1906, seven cells made in 1932, and 26 cells made in 1948. Long-term stability of the volt reference was also maintained by comparisons of neutral and acid cells, preparing and characterizing new cells, and through international comparisons and absolute ampère and ohm experiments.⁸ The use of the Weston cell as the national standard of voltage was supported by a considerable amount of research in electrochemistry and related fields. However, there were still problems with the standard cells. In the late 1960s the relative deviation of the output voltages of the individual national standards could be determined with an accuracy of less than 1 μ V. However, the values deviated from each other by more than 10 μ V. This clearly demonstrated

¹L. Galvani, *De Virebus Electricitatis in Motu Musculari Commentarius* (1791).

²W. Ostwald, *Elektrochemie, ihre Geschichte und Lehre* (1896).

³**John Frederic Daniell**, British chemist and meteorologist, born March 12, 1790 in London, England; died March 13, 1845 in London, England.

⁴J.F. Daniell, *Philosophical Transactions of the Royal Society* (1886).

⁵**Edward Weston**, born May 9, 1850, died August 20, 1936, English chemist noted for his achievements in electroplating and his development of the battery, named the Weston cell, for the voltage standard.

⁶F. B. Silsbee, *Establishment and Maintenance of the Electrical Units*, NBS Circular 475, National Bureau of Standards, Washington, DC (1949).

⁷Walter J. Hamer, *Standard Cells – Their Construction, Maintenance, and Characteristics*, NBS Monograph 84, National Bureau of Standards, Washington, DC (1965).

⁸R. L. Driscoll and P. T. Olsen, *Application of nuclear resonance to the monitoring of electrical standards*, in *Precision Measurement and Fundamental Constants*, D. N. Langenberg and B. N. Taylor (eds.), NBS Special Publication 343, National Bureau of Standards, Washington, DC (1971), pp. 117-121.



Figure 6.1: The Weston cell. Weston invented and patented the saturated cadmium cell in 1893. It had the advantage of being less temperature sensitive than the previous standard, the Clark cell. It also had the advantage of producing a voltage very near to one volt: 1.0183 V.

the necessity of a new voltage standard providing better accuracy and less deviations between of the various national standards.

We note that in 1948 the *International Units* were replaced by the *Absolute Units – meter, kilogram, second, ampère (MKSA)*. In this system, the voltage is a derived quantity and its unit must be determined by an experiment, for example, by a voltage balance, which links it to the MKSA system. Accordingly, a standard cell became a laboratory realization of the unit volt. The system of absolute units was adopted unchanged by the *Système International (SI)*, which was introduced by the Conférence Générale des Poids et Mesures in 1960.

In the late 1950s, research in solid-state physics stimulated the growth of the semiconductor industry. A new type of voltage standard based on a solid-state device, the *Zener diode*, appeared in the early 1960s. **W. G. Eicke** at NBS first reported the possibility of using Zener diodes as transport standards.⁹ In the following years, after several manufacturers started making commercial Zener voltage standards, these references began to replace standard cells in commercial use. Although Zener voltage standards exhibit higher noise characteristics than standard cells and are affected by environmental conditions such as temperature, atmospheric pressure, and relative humidity, they are now widely used in many metrology laboratories because of their robust transportability.

6.1.2 Quantum Standards for Electrical Units

The realization of physical units by systems like the standard cells implies a number of problems such as (i) damaging by improper handling, (ii) dependence on external parameters, and (iii) difficult comparison due to transport problems. In contrast, devices based on quantum effects could reduce the realization of a physical unit to the determination of fundamental constants, which are – as far as we know – independent of time and space. In the case of a quantum representation of a physical unit, the calibration can be decentralized because the unit can be reproduced with fundamental accuracy in every laboratory. Then, a regular comparison of standards is no longer necessary.

Due to the obvious advantages of quantum standards, there have been considerable efforts over the past decades to realize the physical units by quantum devices. For example, much progress has been made in the laser supported realization of the unit of length and the realization of the electrical units on the basis of the following quantum effects:

⁹W. G. Eicke, *Commentaires sur l'utilisation des diodes de zener comme etalons de tension*, Comité Consultatif d'Électricité, 11e Session, BIPM, Paris, France (1963), pp. 1874-1877.

- *Josephson Effect*¹⁰
- *Quantum Hall Effect*^{11,12}
- *Single Charge Tunneling Effect*^{13,14}

According to the second Josephson equation

$$V = \frac{h}{2e} f = \Phi_0 f, \quad (6.1.1)$$

the Josephson effect reduces the determination of a voltage V to the precise counting of the number of flux quanta Φ_0 crossing the junction. To ensure that all standard laboratories can take full advantage of the small uncertainty in the realization of the “quantum volt”, the *Consultive Committee of Electricity (CCE)*, recommended the following value for the Josephson constant in 1989¹⁵

$$K_{J-90} \equiv \left(\frac{h}{2e} \right)^{-1} = \frac{1}{\Phi_0} = 483\,597.9 \text{ GHz/V} . \quad (6.1.2)$$

This value is in use since January 1990. In the same way, according to

$$I = e f \quad (6.1.3)$$

the single charge tunneling effect reduces the determination of a current to the precise counting of single electrons tunneling from one electrode to the other. Although the determination of a current by counting electrons is studied intensively since about 1990, this method still suffers from the difficulties in fabricating the required nano-circuits.

Based on the quantum Hall effect also the ohm can be established based on a quantum effect. The von Klitzing constant $R_K = \frac{h}{e^2}$ was defined by the CCE in 1990 to

$$R_{K-90} \equiv \frac{h}{e^2} = 25\,812.802 \, \Omega . \quad (6.1.4)$$

The Quantum Triangle for Electrical Units

The relations between the electrical units according to the quantum definition are shown in Fig. 6.2. They are interrelated by the so-called *quantum mechanical triangle*. We note that the analogy between the determination of voltage and current – the counting of flux and charge quanta – results from the fact

¹⁰B.D. Josephson, *Possible new effects in superconducting tunneling*, Phys. Lett. **1**, 251-253 (1962).

¹¹K. von Klitzing, G. Dorda, M. Pepper, *New method for high accuracy determination of the fine-structure constant based on quantized Hall resistance*, Phys. Rev. Lett. **45**, 494-497 (1980).

¹²K. von Klitzing, *The quantized Hall effect*, Rev. Mod. Phys. **58**, 519-531 (1986).

¹³L.J. Geerlings *et al.*, *Frequency locked turnstile device for single electrons*, Phys. Rev. Lett. **64**, 2691-2694 (1990).

¹⁴K.K. Likharev, *Correlated discrete transfer of single electrons in ultra-small tunnel junctions*, IBM J. Res. Develop. **32**, 144-158 (1988).

¹⁵T.J. Quinn, *News from the BIPM*, Metrologia **26**, 69-74 (1989).

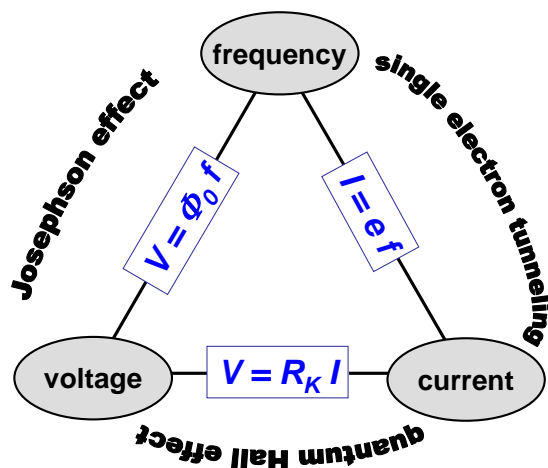


Figure 6.2: The metrological triangle for the electrical units. Josephson effect and single electron tunneling effect relate the units for voltage and current with that of the frequency. Voltage and current are linked via the quantum Hall effect.

that magnetic flux and electric charge are dual quantities from the viewpoint of quantum mechanics.¹⁶ Fig. 6.2 demonstrates that it would be important to close the triangle experimentally by the precise determination of the current via charge counting. This could be important for the redefinition of the international system of physical constants and might result in the clarification of discrepancies in the determination of the fine structure constant.^{17,18}

¹⁶A.J. Leggett, *Macroscopic Quantum Systems and the Quantum Theory of Measurement*, Suppl. Theor. Phys. **69**, 80-100 (1980).

¹⁷B.N. Taylor, *The possible role of the fundamental constants in replacing the kilogram*, IEEE Trans. Instrum. Meas. **IM-40**, 86-91 (1991).

¹⁸B.N. Taylor, E.R. Cohen, *How accurate are the Josephson and quantum Hall effects and QED*, Phys. Lett. **153 A**, 308-312 (1991).

6.2 The Josephson Voltage Standard

6.2.1 Underlying Physics

The physics underlying the Josephson voltage standard already has been discussed in Chapter 3. As we have seen in section 3.3, the dynamics of the phase difference φ across a Josephson junction can be locked to an external oscillator. In this case the supercurrent is forced to oscillate at the frequency $f_1 = 2\pi\omega_1$ of the external oscillator or at higher harmonics nf_1 over a considerable range of the applied dc current. This effect results in a series of constant voltage steps in the current-voltage characteristics (IVCs) of the junction, the so-called Shapiro steps,¹⁹ at the voltages (compare (3.3.26) in section 3.3.3)

$$V_n = n \frac{h}{2e} f_1 = n \Phi_0 f_1 \quad n = 1, 2, 3, \dots \quad (6.2.1)$$

For a specific n the dc current range $|\langle I_s \rangle_n|$ of the n^{th} voltage step is given by the n^{th} order Bessel function \mathcal{J}_n (compare (3.3.27) in section 3.3.3)

$$|\langle I_s \rangle_n| = I_c \left| \mathcal{J}_n \left(\frac{2eV_1}{hf_1} \right) \right| \quad (6.2.2)$$

Here, V_1 is the amplitude of the external high-frequency voltage source. The maximum current width of the n^{th} step can be obtained by properly choosing the argument that maximizes the Bessel function, i.e. the amplitude V_1 of the microwave radiation. The dependence $\mathcal{J}_n \left(\frac{2eV_1}{hf_1} \right)$ has been shown in Fig. 3.11.

Equation (6.2.1) for V_n forms the physical basis of the Josephson voltage standard. It has been proven experimentally with very high precision.^{20,21,22} Fig. 6.3 shows a sketch of an underdamped planar SIS-type Josephson junction together with the IVCs under microwave radiation. It is seen that the constant voltage steps are crossing the voltage axis leading to the so-called zero-current constant voltage steps.

6.2.2 Development of the Josephson Voltage Standard

Single Junction Standards

Soon after the prediction of the Josephson effect the voltage-frequency relation $V = \Phi_0 f$ was experimentally confirmed with high precision. One of the early issues was whether this relationship was material independent. In 1968 **Clarke** as well as **Parker, Langenberg, Denenstien**, and **Taylor** compared, via a potentiometer, the Josephson voltages of junctions consisting of five different superconducting materials and various combinations of thin-film tunnel junctions or point contacts with 1.018 V Weston saturated

¹⁹S. Shapiro, Phys. Rev. Lett. (1963).

²⁰R.L. Kautz, L. Lloyd, *Precision of series array Josephson voltage standards*, Appl. Phys. Lett. **51**, 2043-2045 (1987).

²¹J. Niemeyer, L. Grimm, C.A. Hamilton, R.L. Steiner, *High precision measurement of a possible resistive slope of Josephson array voltage steps*, IEEE Electron Dev. Lett. **EDL-7**, 44-46 (1986).

²²J.-S. Tsai, A.K. Jain, J.E. Lukens, *High precision test of the universality of the Josephson voltage-frequency relation*, Phys. Rev. Lett. **51**, 316-318 (1983).

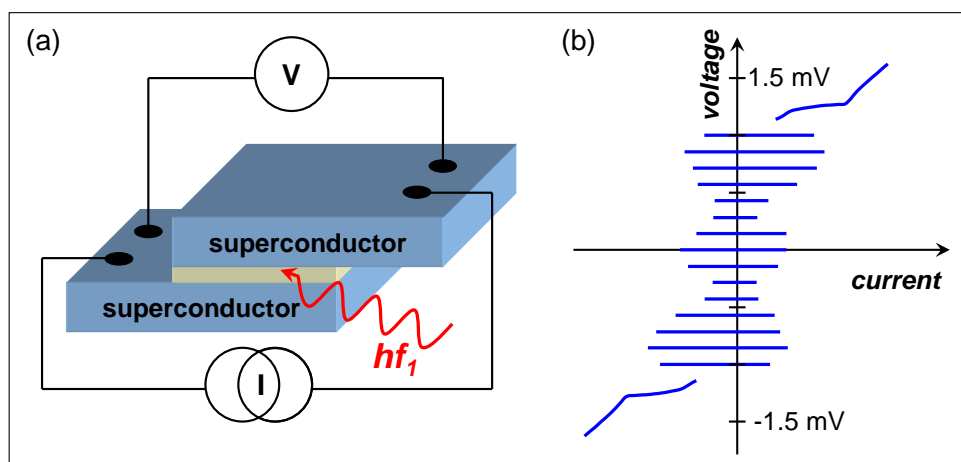


Figure 6.3: (a) Sketch of a planar SIS-type Josephson junction. (b) IVC of an underdamped Josephson junction under microwave irradiation ($f_1 = 35$ GHz). The Shapiro steps cross the voltage axis resulting in zero current constant voltage steps.

standard cells.^{23,24,25} They obtained a value of $2e/h$ with a one-standard-deviation fractional uncertainty of 3.6×10^{-6} . The use of SQUID null detectors in the early 1970s allowed this to be tested to a few parts in 10^9 , and thus the Josephson effect had obvious potential for use as a voltage standard.²⁶

As indicated by Fig. 6.3, the maximum available voltage of the current steps is of the order of 1 mV for a single Josephson junction. Therefore, precise voltage dividers have to be developed to compare the Josephson voltage standard to the electrochemical standard cells. By the early 1970s, the mV-range Josephson junction voltages could be compared with 1.018 V standard cells to a few parts in 10^8 .^{27,28} International comparisons in 1971-72 among national metrology institutes found that the measured values of $2e/h$ agreed with each other to within 2×10^{-7} .²⁹ These results suggested the course of adopting a value of $2e/h$ for use in maintaining units of voltage. Consequently, in 1972 the CCE suggested to use a value of $K_{J-72} = 2e/h = 483\,594.0$ GHz/V for voltage comparison.³⁰ This value was corrected to $K_{J-90} = 483\,597.9$ GHz/V in 1990. Since that time the national voltage standards have been controlled by single Josephson junction voltage standards and the role of the Weston cell as the primary standard for the volt has ended. Besides the relative insensitivity against environmental influences, the new Josephson voltage standard had a better reproducibility of only a few parts in 10^8 , which resulted in a considerable reduction of the spread of the standard voltages of the different national laboratories (cf. Fig. 6.4).³¹

²³J. Clarke, *Experimental comparison of the Josephson voltage-frequency relation in different superconductors*, Phys. Rev. Lett. **21**, 1566-1569 (1968).

²⁴W. H. Parker, D. N. Langenberg, A. Denenstein, and B. N. Taylor, *Determination of e/h using macroscopic quantum phase coherence in superconductors: I. Experiment*, Phys. Rev. **177**, 639-664 (1969).

²⁵T.D. Bracken, W.O. Hamilton, *Comparison of the microwave induced constant voltage steps in Pb and Sn Josephson junctions*, Phys. Rev. **B 6**, 1603-2609 (1972).

²⁶B. N. Taylor, W. H. Parker, D. N. Langenberg, and A. Denenstein, *On the use of the ac Josephson effect to maintain standards of electromotive force*, Metrologia **3**, 89-98 (1967).

²⁷F. K. Harris, H. A. Fowler, and P. T. Olsen, *Accurate Hamon-pair potentiometer for Josephson frequency-to-voltage measurements*, Metrologia **6**, 134-142 (1970).

²⁸B. F. Field, T. F. Finnegan, and J. Toots, *Volt maintenance at NBS via $2e/h$: a new definition of the NBS volt*, Metrologia **9**, 155-166 (1973).

²⁹Woodward G. Eicke and Barry N. Taylor, *Summary of international comparisons of as-maintained units of voltage and values of $2e/h$* , IEEE Trans. Instrum. Meas. **IM-21**, 316-319 (1972).

³⁰J. Terrien, *New from the Bureau International des Poids et Mesures*, Metrologia **9**, 40-43 (1973).

³¹B.W. Petley, *Quantum metrology and electrical standards: the measurement of $2e/h$* , Quantum Metrology and Fundamental Physical Constants, NATO ASI Series B, Vol. **98**, P.H. Cutler and A.A. Lucas eds., Plenum, New York (1983).

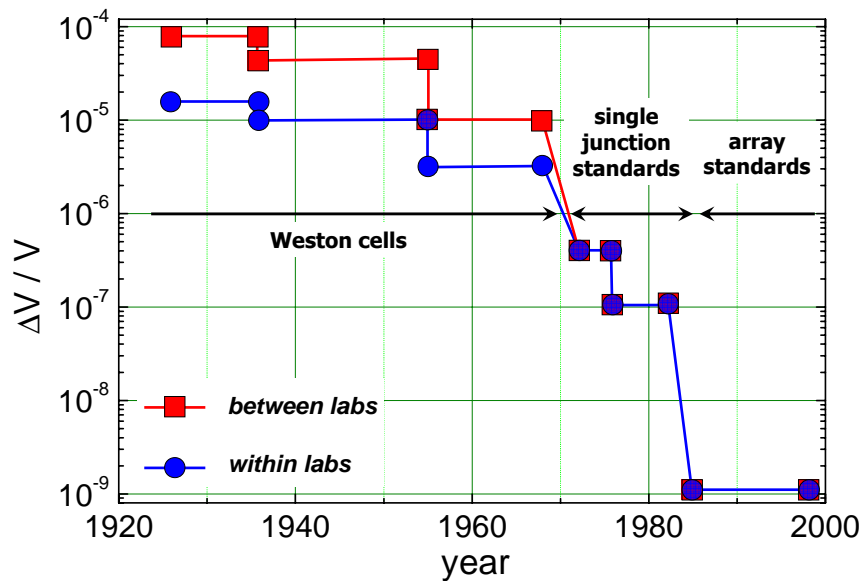


Figure 6.4: Results of the international voltage comparisons between 1920 and 2000 performed by several national laboratories. The relative accuracy $\Delta V/V$ has been improved from about 10^{-4} to 10^{-9} going from Weston cells to series array Josephson voltage standards (data from H. Bachmair, PTB Bericht **E-24**, 1 (1988), and C. A. Hamilton and Y. H. Tang, *Metrologia* **36**, 53-58 (1999)).

Series Array Standards

Despite the fact that the Josephson junctions provided undoubtedly better references than standard cells, some problems remained. The typical 5 mV to 10 mV reference output from early Josephson devices made from a few junctions required both very low-level voltage balances and scaling by a factor of 100, both of which seriously limited the accuracy of measuring 1.018 V standard cells. To overcome these difficulties attempts to use series arrays of Josephson junctions were made to obtain larger reference voltages.³² However, that time the junction fabrication was not reliable enough to guarantee parameter spreads that would have allowed to bias a large series array of junctions with a single current source. Nevertheless, reference voltages up to 100 mV with an uncertainty of a few parts in 10^9 have been obtained.

Then in 1977, **M.T. Levinson** and colleagues showed that unbiased Josephson junctions spontaneously develop quantized dc voltages when irradiated with microwaves. Using the zero current steps, arrays can tolerate much larger spread in the junction parameters because they can be operated at zero current, where all the junctions have steps.³³ Stable 1 V zero-crossing arrays were operating at National Bureau of Standards (NBS)³⁴ and the Physikalisch-Technische Bundesanstalt (PTB)³⁵ by 1985, using about 1500 junctions and rf fields of 70 GHz to 90 GHz. Arrays with output voltages at the level of 1 V soon were used worldwide.³⁶ Note that for an operation frequency of 70 GHz Shapiro steps at multiples of about $145 \mu\text{V}$ are obtained. That is, in order to obtain a total output voltage of 1 V, about 7 000 junctions are

³²T. Endo, M. Koyanagi, A. Nakamura, *High accuracy Josephson potentiometer*, IEEE Trans. Instrum. Meas. **IM-32**, 267-271 (1983).

³³M.T. Levinson, R.Y. Chiao, M.J. Feldman, B.A. Tucker, *An inverse ac Josephson effect voltage standard*, Appl. Phys. Lett. **31**, 226-278 (1977).

³⁴C. A. Hamilton, R. L. Kautz, R. L. Steiner, and Frances L. Lloyd, *A Practical Josephson Voltage Standard at 1 V*, IEEE Electron Device Lett. **EDL-6**, 623-625 (1985).

³⁵J. Niemeyer, L. Grimm, W. Meier, J. H. Hinken, and E. Vollmer, *Stable Josephson reference voltages between 0.1 and 1.3 V for high-precision voltage standards*, Appl. Phys. Lett. **47**, 1222-1223 (1985).

³⁶Richard L. Steiner and Bruce F. Field, *Josephson array voltage calibration system: operational use and verification*, IEEE Trans. Instrum. Meas. **38**, 296-301 (1989).

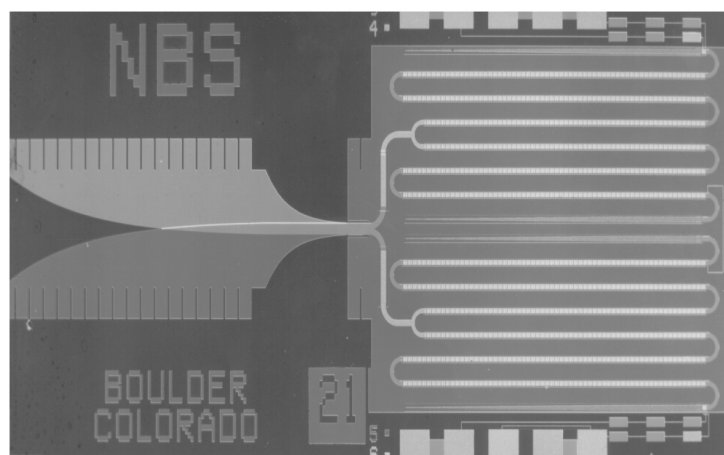


Figure 6.5: One-Volt Josephson junction array consisting of 3020 Josephson junctions (courtesy of NIST, Boulder).

required, if the junctions are operated at $n = 1$ Shapiro step. For $n = 5$, still about 1 400 junctions are required. Fig. 6.5 shows an optical micrograph of a 1 V series array consisting of 3020 junctions. The difficulties that have to be solved in the realization of series array Josephson voltage standards are the following:

- ***Fabrication of a large number of Josephson junctions with almost identical parameters***

If there is for example a too large spread of the critical current values $I_{c,i}$ of the Josephson junctions, there is a certain probability that not all junctions are operated at the same Shapiro step, since they are biased with the same dc current resulting in different values for $I_{\text{bias}}/I_{c,i}$. This problem has been solved by both improving the fabrication process, by optimizing the junction parameters (see section 6.2.3) and by using zero-current steps in arrays of underdamped junctions.

Voltage standard chips are typically fabricated on silicon or glass substrates with the integrated circuit consisting of eight levels: (1) a 300 nm thick Nb ground plane, (2) a $2\ \mu\text{m}$ layer of SiO_2 that forms the microstripline dielectric, (3) a 200 nm Nb film that forms the lower electrode of the Josephson junctions, (4) a 3 nm metal oxide layer that forms the Josephson tunneling barrier, (5) a 100 nm Nb junction counterelectrode, (6) a 300 nm SiO_2 film with windows for contacts to the counterelectrode, (7) a 400 nm film of Nb that connects the junction counterelectrodes, and (8) a 100 nm resistive film that forms the stripline terminations. This structure is shown in Fig. 6.6, however, with the superconducting groundplane on top instead at bottom.

- ***Homogeneous microwave irradiation***

Each Josephson junction in the series array should be irradiated by the same microwave power. Therefore, the proper design of the microwave circuit is an important aspect of series array Josephson voltage standards. Usually, the Josephson junctions are arranged in a series array that is incorporated into a superconducting microwave stripline as shown in Fig. 6.6. In this way an effective and uniform coupling of the microwave to the single junctions could be obtained and large arrays with more than 15 000 junctions for reference voltages above 10 V could be realized.^{37,38} Due to the finite damping of the microwave signal along the microwave stripline sketched in Fig. 6.6, a homogeneous microwave irradiation is still difficult to achieve for large series arrays of several

³⁷F.L. Lloyd, C.A. Hamilton, J.A. Beall, D. Go, R.H. Ono, R.E. Harris, *A Josephson array voltage standard at 10 V*, IEEE El. Dev. Lett. **EDL-8**, 449-450 (1987).

³⁸R. Pöpel, J. Niemeyer, R. Frommknecht, W. Meier, L. Grimm, *1- and 10-V series array Josephson voltage standard in Nb/ AlO_x /Nb technology*, J. Appl. Phys. **68**, 4294-4303 (1990).

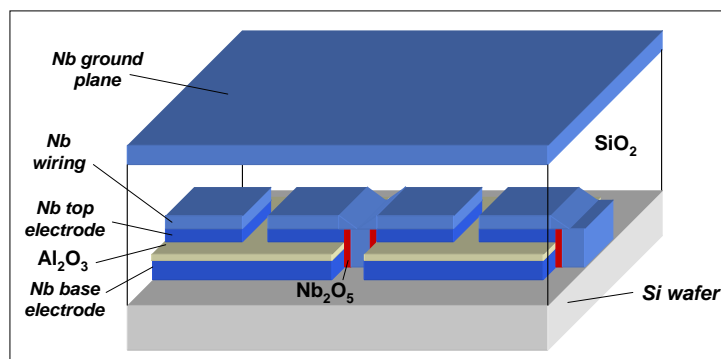


Figure 6.6: Sketch of a small part of a Josephson series array embedded into a microwave stripline.

thousands of junctions. This problem has been solved by using a meander-shaped design of the array. For the microwave signal, the different parts of the array are in parallel, whereas for the dc signal they are still in series. The microwave design and an optical micrograph of a chip with a series array Josephson voltage standard is shown in Fig. 6.7. A fin-line taper inserted into a slit in a waveguide is often used as microwave antenna. The antenna structure is then connected to a microwave divider and blocking capacitors. Each microwave path is terminated by a lossy line to prevent microwave reflections from the end, which would cause a standing wave pattern and hence an inhomogeneous microwave distribution. With respect to the dc connections, the four lines in Fig. 6.7a are connected in series. With some variations this design is used by most manufactures worldwide.^{39,40}

In the 1980s series arrays with a continuously growing number of junctions have been developed mainly at NIST, Boulder, and PTB, Braunschweig.^{41,42} With arrays containing about 15 000 Josephson junctions about 150 000 quantized voltage values spanning the range from -10 V to +10 V could be realized. By 1989, all of the hardware and software for a complete voltage metrology system were commercially available. The widespread use of Josephson junction arrays in national standards laboratories, and better SI determinations of $2e/h$, led the CCE to recommend a new exact conventional value for the Josephson constant: $K_{J-90} = 483\,597.9\text{ GHz/V}$, which is fractionally larger by 8×10^{-6} than the 1972 conventional value. The new value was adopted worldwide on January 1, 1990. This definition of K_{J-90} is the present volt representation, based on an ideal Josephson voltage standard. The conventional value was assumed by the CCE to have a relative standard uncertainty of $0.4\ \mu\text{V/V}$. By convention, this uncertainty is not included in the uncertainties of the representation of the volt, since any offset from the SI volt will be consistent among different laboratories using the Josephson effect standard. Today, there are Josephson array voltage standards in more than 50 national, industrial, and military standards laboratories around the world. A program of international comparisons carried out by the Bureau International des Poids et Mesures (BIPM) has measured differences between a traveling Josephson standard and those of the National Measurement Institutes that are typically less than 1 part in 10^9 .^{43,44,45,46}

³⁹C.A. Hamilton, C.J. Burroughs, R.L. Kautz, *The performance and reliability of the NIST 10 V Josephson array*, IEEE Trans. Instrum. Meas. **IM-44**, 233-241 (1995).

⁴⁰S.B. Kaplan, *Technology transfer and the Josephson voltage standard*, Supercond. Industry **8**, 25-30 (1995).

⁴¹C.A. Hamilton, *Josephson voltage standards*, Rev. Sci. Instrum. **71**, 3611-3623 (2000).

⁴²J. Niemeyer, PTB Mitteilungen **110**, 169 (2000).

⁴³D. Reymann and T. J. Witt, IEEE Trans. Instrum. Meas. **42**, 596 (1993).

⁴⁴J. P. Lo-Hive, D. Reymann, and G. Geneve's, IEEE Trans. Instrum. Meas. **44**, 230 (1995).

⁴⁵D. Reymann, T. J. Witt, G. Eklund, H. Pajander, and H. Nilsson, IEEE Trans. Instrum. Meas. **46**, 220 (1997).

⁴⁶D. Reymann, T. J. Witt, G. Eklund, H. Pajander, H. Nilsson, R. Behr, T. Funck, and F. Müller, IEEE Trans. Instrum. Meas. **48**, 257 (1999).

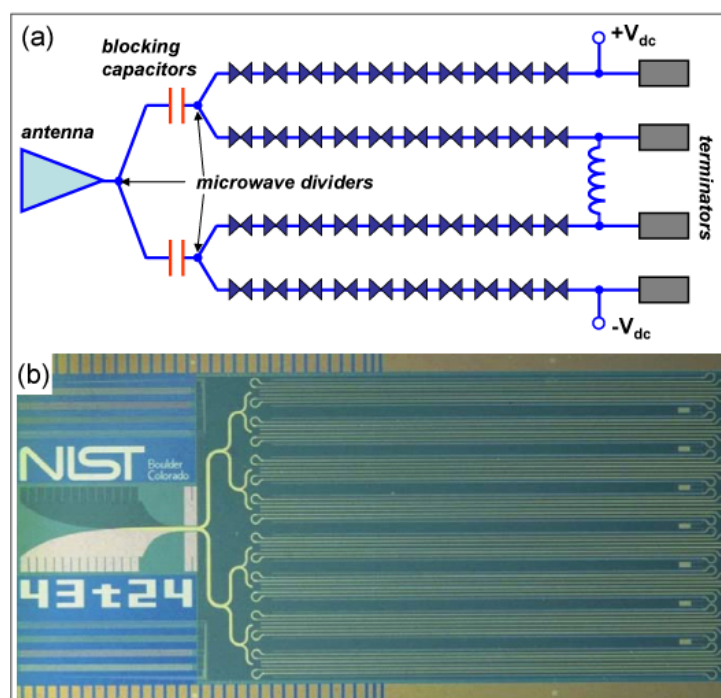


Figure 6.7: (a) Schematics of the microwave design of a series array Josephson voltage standard. (b) Optical micrograph of a NIST series array Josephson voltage standard for 10 V. The array consist of 20 208 Josephson junctions operated at 75 GHz. On the left the fin-line taper is seen. The series array on the right is split up into 16 parallel parts with 1 263 junctions each (courtesy of NIST, Boulder).

6.2.3 Junction and Circuit Parameters for Series Arrays

The idea of using series arrays for the realization of Josephson voltage standards with higher reference voltage is simple. By the use of N junctions in series the output voltage can be increased to N times the value available for a single junction. However, a prerequisite for the generation of stable zero current steps is that the phase lock of the phase dynamics of the nonlinear Josephson junction and the external microwave oscillator must be maintained during the calibration process. This condition must now be satisfied for a large series array and not only a single junction. In order to achieve this goal, reduction of external noise sources is required and one also has to avoid to operate the Josephson junctions in a regime where chaotic phenomena can occur.

The parameter regime of single Josephson junctions where optimum phase locking is guaranteed has been analyzed by **Kautz** as well as **Nöldecke** and coworkers.^{47,48} They found the following conditions for the frequency $f_1 = 2\pi\omega_1$ of the external microwave oscillator:

$$\omega_1 \gg \omega_p = \sqrt{\frac{2eI_c}{\hbar C}} = \sqrt{\frac{2eJ_c}{\hbar C_s}}. \quad (6.2.3)$$

Here, ω_p is the plasma frequency, $J_c = I_c/A$ is the critical current density and $C_s = C/A$ the specific junction capacitance. We see that one has to use junctions with low plasma frequency, i.e. low critical current density and large specific capacitance and/or high microwave frequencies.

⁴⁷R.L. Kautz, *Noise, chaos and the Josephson effect*, Rep. Prog. Phys. **59**, 935-992 (1996).

⁴⁸Ch. Noeldeke, R. Gross, M. Bauer, G. Reiner, H. Seifert, *Experimental Survey of Chaos in the Josephson Effect*, J. Low Temp. Phys. **64**, 235 (1986).

In order to obtain a homogeneous distribution of the rf current and in order to avoid large junction effects, the junction length L and width W must satisfy the conditions:

$$L < \frac{3}{\omega_1} \frac{1}{\sqrt{n\mu_0 C_s(t + 2\lambda_L)}} = L_{\max} \quad (6.2.4)$$

$$L, W < \frac{\pi}{\omega_1} \frac{1}{\sqrt{\mu_0 C_s(t + 2\lambda_L)}} = W_{\max} . \quad (6.2.5)$$

Here, t is the thickness of the tunneling barrier, λ_L the London penetration depth of the electrode material and n the number of the constant voltage step.⁴⁹

Detailed simulations have shown that the microwave frequency ω_1 should be larger than about $3\omega_p$ in order to avoid the regime of chaotic phase dynamics. This results in an upper limit of

$$J_{c,\max} = \frac{9\omega_1^2 \hbar C_s}{2e} . \quad (6.2.6)$$

Together with the limitations on the junction length and width this leads to a maximum value of the critical current $I_{c,\max} = J_{c,\max} W_{\max} L_{\max}$ and thus according to (6.2.2) to a maximum width of the constant voltage steps, over which a stable operation of the voltage standard can be achieved. For the commonly used Nb/AlO_x/Nb junction technology we have $C_s \simeq 6 \mu\text{F}/\text{cm}^2$ and $\lambda_L \simeq 80 \text{ nm}$. At $f_1 = 70 \text{ GHz}$ this results in $J_{c,\max} \simeq 40 \text{ A}/\text{cm}^2$, $W_{\max} \simeq 65 \mu\text{m}$, $L_{\max} \simeq 20 \mu\text{m}$, and hence $I_{c,\max} \simeq 500 \mu\text{A}$. The maximum step width for the 7th voltage step is then about $350 \mu\text{A}$.⁵⁰

⁴⁹R.L. Kautz, G. Costabile, *A Josephson voltage standard using a series array of 100 junctions*, IEEE Trans. Magn. **MAG-17**, 780-783 (1981).

⁵⁰J. Niemeyer, *Josephson voltage standards*, in *Handbook of Applied Superconductivity 2*, B. Seeber ed., Institute of Physics Publishing, Bristol (1998), pp.1813-1834.

6.3 Programmable Josephson Voltage Standard

In the previous section we have discussed Josephson voltage standards based on zero-current voltage steps. These steps are obtained for series arrays or single underdamped junctions. It is obvious from Fig. 6.3 that a particular problem with these steps is their strong overlapping making the rapid switching between the steps problematic. This problem is sketched in Fig. 6.8. In order to access a certain Shapiro step, that is a specific output voltage V_{out} , one could simply think of applying a dc voltage $V_b \simeq V_{\text{out}}$ using e.g. a battery. However, due to the finite resistance of the leads to the chip, the voltage is split up between the array and the leads following the loadline as shown in Fig. 6.8. Since the loadline is crossing several Shapiro steps, it is difficult to select a specific step in a well defined way. It is evident that there are different ways of splitting up the voltage between the leads and the array. Once a specific step is adjusted, the step voltage has to be measured by a voltmeter that has an accuracy sufficient to distinguish between neighboring steps (about $145 \mu\text{V}$ for 70 GHz).

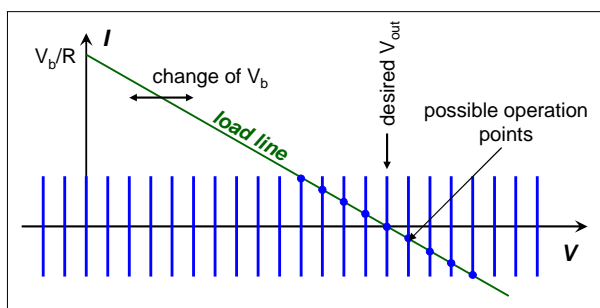


Figure 6.8: Sketch of the adjustment procedure for the quantized Shapiro step voltages in a series array of underdamped Josephson junctions. The external battery voltage V_b can be distributed along the load line V_b/R in different ways on the leads and the series array.

The problem sketched in Fig. 6.8 can be avoided by using overdamped Josephson junctions. In principle, overdamped Josephson junctions can be obtained by shunting underdamped SIS-type junctions with an external resistor. However, this makes the fabrication process more complicated. More appropriate are SNS-type (superconductor/normal/superconductor) or SINIS-type (superconductor/insulator/normal/insulator/superconductor) Josephson junctions. As shown by Fig. 6.9, in these overdamped junctions the steps do not overlap and one can rapidly select a specific step by adjusting the bias current.

Series arrays of overdamped junctions can be used to realize programmable Josephson voltage standards. Such systems use a series array of nonhysteretic junctions with IVCs as shown in Fig. 6.9, which are divided into a binary sequence as schematically shown in Fig. 6.10. The microwave excitation for each junction is set to roughly equalize the amplitude of the $n = 0$ and $n = 1$ constant voltage steps. Each segment of the array can be set to the $n = 1$, 0 , or $+1$ steps by applying a bias current ($-I_1$, $I_0 = 0$, $+I_1$) corresponding to the middle of the corresponding steps (cf. Fig. 6.9). The combined step number N for the whole array can thus be set to integer values between $-M$ and $+M$, where M is the total number of junctions in the array.^{51,52,53} The rapid settling time, the inherent step stability, and the large operating current margins of the Josephson voltage standard sketched in Fig. 6.10 make it superior to a conventional Josephson voltage standard for many dc measurements. The improved performance of

⁵¹C.A. Hamilton, C.J. Burroughs, and R.L. Kautz, *Josephson D/A Converter with Fundamental Accuracy*, IEEE Trans. Instrum. Meas. **44**, 223-225 (1995).

⁵²C.A. Hamilton, C.J. Burroughs, R.L. Kautz, *Digital-to-Analog Converter with Voltage defined by Josephson Frequency Voltage Relation*, U.S. Patent No. 5565866, Oct. 1996.

⁵³C.A. Hamilton, C.J. Burroughs, S.P. Benz, and J.R. Kinard, *AC Josephson Voltage Standard: A Progress Report*, IEEE Trans. Instrum. Meas. **46**, 224-227 (1997).

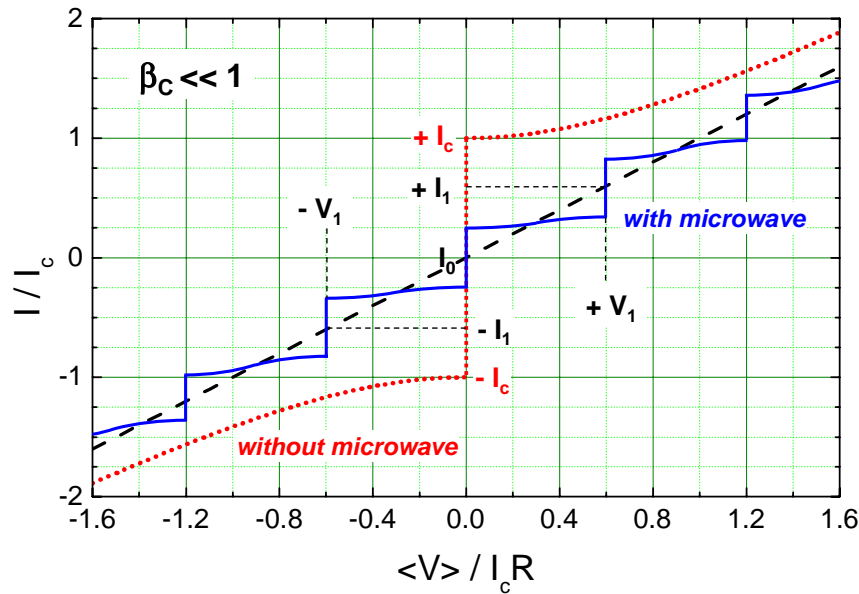


Figure 6.9: IVC of an overdamped ($\beta_c \ll 1$) Josephson junction with (solid line) and without (dotted line) microwave irradiation. The dashed curve shows the ohmic line.

programmable Josephson voltage standards has been made possible by a new integrated-circuit technology using intrinsically shunted SNS- or SINIS-type Josephson junctions. These junctions have been fabricated by extending the Nb/AIO_x/Nb technology. However, also intrinsically overdamped junctions of the high temperature superconductors could be used, although at present the parameter spread of these junctions is still too large.⁵⁴ An important fact is that the overdamped junctions operate at lower excitation frequencies (10 to 20 GHz)⁵⁵ than those of Josephson voltage standards based on hysteretic SIS junctions and have about 100 times larger step amplitudes (typically 2 to 4 mA).⁵⁶ The only disadvantage of the programmable Josephson voltage standard is the required larger number of Josephson junctions, because only the first voltage step is contributing to the sum voltage. Typically, the number of junctions must be increased by a factor of five to seven.

For a microwave frequency of 20 GHz the voltage generated by each step is $V = f/K_{J-90} \simeq 41.3 \mu\text{V}$. Then, about 24 000 junctions are required to achieve a total output voltage of about 1 V. For example, a binary array consisting of segments from 2^0 to 2^{14} junctions would consist of $2^{15} - 1 = 32\,367$ individual junctions and would yield a maximum output voltage of about 1.35 V at a driving frequency of 20 GHz. Programmable voltage standards for the 1 V level have been successfully fabricated by NIST, Boulder, using Josephson junctions with a normal conducting barrier of AuPd alloy,⁵⁷ and by PTB using Josephson junctions with a superconductor-insulator-normal conductor-insulator-superconductor (SINIS) structure.⁵⁸

Since the Zener reference secondary voltage standards commonly used provide reference voltages of 1 and 10 V, there is a demand for an intrinsically stable and rapidly programmable voltage standard for the 10 V level. If microwaves in the frequency range of 70 GHz are used, a series array of about 70 000 junctions is required, which must be fabricated with low parameter spread and small defect rate. The

⁵⁴A.M. Klushin, S.I. Borovitskii, C. Weber, E. Sodtke, R. Semerad, W. Prusseit, V.D. Gelikonova, H. Kohlstedt, *Appl. Supercond.* **158**, 587 (1997).

⁵⁵R.L. Kautz, *Quasipotential and the stability of phase lock in nonhysteretic Josephson junctions*, *J. Appl. Phys.* **76**, 5538-5544 (1994).

⁵⁶S.P. Benz, *Superconductor-normal-superconductor Junctions for Programmable Voltage Standards*, *Appl. Phys. Lett.* **67**, 2714-2716 (1995).

⁵⁷S.P. Benz, C.A. Hamilton, C.J. Burroughs, T.E. Harvey, and L.A. Christian, *Appl. Phys. Lett.* **71**, 1866 (1997).

⁵⁸R. Behr, H. Schulze, F. Müller, J. Kohlmann, and J. Niemeyer, *IEEE Trans. Instrum. Meas.* **48**, 270 (1999).

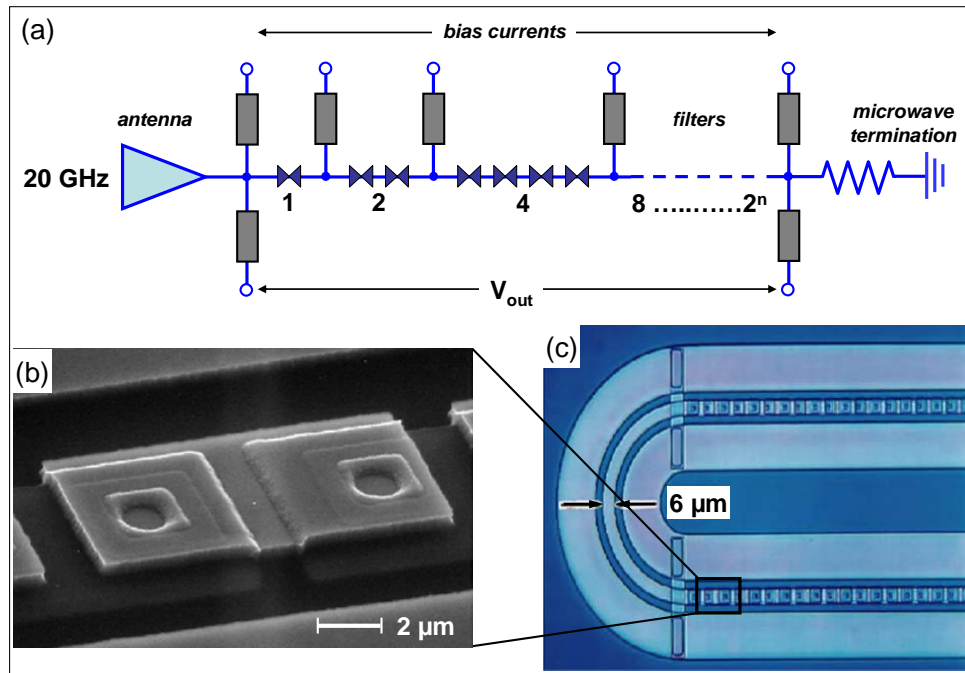


Figure 6.10: (a) Sketch of the arrangement and bias schematic of a programmable Josephson voltage standard. (b) Scanning electron microscopy image showing the $2 \times 2 \mu\text{m}^2$ Nb/PdAu/Nb Josephson junctions of a 32 768 Josephson junction series array. The series array is arranged in several segments connected with coplanar waveguides. In (c) a small section of the coplanar waveguide with the distribution of junctions along the center conductor is shown (images by courtesy of NIST, Boulder).

whole array must be fed homogeneously with sufficient microwave power. Due to the larger number of junctions required to obtain 10 V using programmable voltage standard arrays, a higher integration density is required to avoid an increase in the chip size. This can be achieved by moderate reduction of the junction area and by a modified microwave design, which is possible because of the different microwave properties of SINIS arrays. Chips with 69 120 SINIS-type Josephson junction series arrays for a programmable 10 V Josephson dc voltage standard have been successfully fabricated and operated with 70 GHz microwave irradiation. The current-voltage characteristics exhibits non-hysteretic voltage steps with a step width of $200 \mu\text{A}$.^{59,60}

6.3.1 Pulse Driven Josephson Arrays

Although the programmable Josephson voltage standards are quite useful in several applications, binary programmable arrays have not been very successful in the synthesis of ac wave forms because the undefined voltage during transitions between steps adds an unacceptable level of uncertainty. To solve this problem, **Benz** and **Hamilton** have developed another approach that biases the array with pulses.⁶¹ So far we only discussed to program the voltage of a Josephson array by changing the step number n resulting in a different voltage $V_n = n f \Phi_0$. It is clear that the same result might be achieved by changing f . Unfortunately, in the case of a sine-wave excitation, the step amplitudes collapse rapidly to zero as the

⁵⁹H. Schulze, R. Behr, J. Kohlmann, F. Müller, and J. Niemeyer, *Design and fabrication of 10 V SINIS Josephson arrays for programmable voltage standards*, *Supercond. Sci. Technol.* **13**, 1293-1295 (2000).

⁶⁰Yonuk Chong, C. J. Burroughs, P. D. Dresselhaus, N. Hadacek, H. Yamamori, and S. P. Benz, *Practical High-Resolution Programmable Josephson Voltage Standards Using Double- and Triple-Stacked MoSi₂-Barrier Junctions*, *IEEE Trans. Appl. Supercond.* **AS-15**, 461-464 (2005).

⁶¹S. P. Benz and C. A. Hamilton, *Appl. Phys. Lett.* **68**, 3171 (1996).

frequency decreases. This means that it is practical to control the voltage via the frequency only over a range of frequency within about a factor of 2 of the optimum frequency $f_c = I_c R / \Phi_0$. However, simulations show that if the sine-wave excitation is replaced with a pulse excitation, then the step amplitude is independent of the pulse repetition frequency for all frequencies below f_c .^{62,63,64} The optimum pulse width is $\tau = 1/\omega_c = 1/2\pi f_c$.

A programmable voltage source based on this idea consists of a single large array of N junctions distributed along a transmission line with wide bandwidth. A pulse train at frequency f propagating down the line generates an average voltage $Nf\Phi_0$ across the ends of the array. A complex output wave form can be generated by modulating the pulse train with a digital word generator. For example, using a clock frequency of $f_c = I_c R / \Phi_0 = 10$ GHz, the pulse sequence 11111000001111100000 creates an output square wave with amplitude $Nf_c\Phi_0$ and frequency 1 GHz.

⁶²R. Monaco, *J. Appl. Phys.* **68**, 679 (1990).

⁶³S. P. Benz, C. A. Hamilton, and C. J. Burroughs, *IEEE Trans. Appl. Supercond.* **AS-7**, 2653 (1997).

⁶⁴F. Liefrink, G. de Jong, P. Teunissen, J. W. Heimeriks, A. Royset, A. A. Dyrseth, H. Schulze, R. Behr, J. Kohlmann, E. Volmer, and J. Niemeyer, *Proc. BEMC* (1999).